



US Army Corps
of Engineers

AD-A226 745

IMPROVEMENT OF OPERATIONS AND MAINTENANCE TECHNIQUES RESEARCH PROGRAM

FILE COPY

TECHNICAL REPORT HL-90-13

CHANNEL MAINTENANCE BY TRAINING STRUCTURES: GUIDANCE FOR NUMERICAL MODEL MESH DEVELOPMENT

by

R. C. Berger, Jr.

Hydraulics Laboratory

DEPARTMENT OF THE ARMY

Waterways Experiment Station, Corps of Engineers
3909 Halls Ferry Road, Vicksburg, Mississippi 39180-6199

DTIC
ELECTE
SEP 28 1990
S B D



September 1990

Final Report

Approved For Public Release; Distribution Unlimited

Prepared for DEPARTMENT OF THE ARMY
US Army Corps of Engineers
Washington, DC 20314-1000

Under Work Unit No. 32350

204

HYDRAULICS



LABORATORY

QUADRILATERAL ELEMENT
PATCH

7	8	9
4	5	6
1	2	3

L
L

Destroy this report when no longer needed. Do not return
it to the originator.

The findings in this report are not to be construed as an official
Department of the Army position unless so designated
by other authorized documents.

The contents of this report are not to be used for
advertising, publication, or promotional purposes.
Citation of trade names does not constitute an
official endorsement or approval of the use of
such commercial products.

Unclassified

SECURITY CLASSIFICATION OF THIS PAGE

REPORT DOCUMENTATION PAGE				Form Approved OMB No. 0704-0188	
1a. REPORT SECURITY CLASSIFICATION Unclassified			1b. RESTRICTIVE MARKINGS		
2a. SECURITY CLASSIFICATION AUTHORITY			3. DISTRIBUTION / AVAILABILITY OF REPORT Approved for public release; distribution unlimited.		
2b. DECLASSIFICATION / DOWNGRADING SCHEDULE					
4. PERFORMING ORGANIZATION REPORT NUMBER(S) Technical Report HL-90-13			5. MONITORING ORGANIZATION REPORT NUMBER(S)		
6a. NAME OF PERFORMING ORGANIZATION USAEWES Hydraulics Laboratory		6b. OFFICE SYMBOL (If applicable) CEWES-HE-P	7a. NAME OF MONITORING ORGANIZATION		
6c. ADDRESS (City, State, and ZIP Code) 3909 Halls Ferry Road Vicksburg, MS 39180-6199			7b. ADDRESS (City, State, and ZIP Code)		
8a. NAME OF FUNDING / SPONSORING ORGANIZATION US Army Corps of Engineers		8b. OFFICE SYMBOL (If applicable)	9. PROCUREMENT INSTRUMENT IDENTIFICATION NUMBER		
8c. ADDRESS (City, State, and ZIP Code) Washington, DC 20314-1000			10. SOURCE OF FUNDING NUMBERS See reverse.		
			PROGRAM ELEMENT NO.	PROJECT NO.	TASK NO.
					WORK UNIT ACCESSION NO.
11. TITLE (Include Security Classification) Channel Maintenance by Training Structures: Guidance for Numerical Model Mesh Development					
12. PERSONAL AUTHOR(S) Berger, R. C., Jr.					
13a. TYPE OF REPORT Final report		13b. TIME COVERED FROM _____ TO _____		14. DATE OF REPORT (Year, Month, Day) September 1990	
15. PAGE COUNT 32					
16. SUPPLEMENTARY NOTATION Available from National Technical Information Service, 5285 Port Royal Road, Springfield, VA 22161.					
17. COSATI CODES			18. SUBJECT TERMS (Continue on reverse if necessary and identify by block number)		
FIELD	GROUP	SUB-GROUP			
			Finite element Resolution		
			Skewness Training structures		
19. ABSTRACT (Continue on reverse if necessary and identify by block number)					
<p>Training structures used to control channel currents and sedimentation, which in the past were designed by rules of thumb, are now frequently the subject of numerical model investigations. The precision and stability of numerical models representing the shallow-water equations and transport generally are strongly influenced by the nature of the computational mesh upon which the calculations take place. This condition is amplified by the presence of man-made structures in the flow. It is therefore imperative that mesh development in the vicinity of these structures be guided so that accurate and reliable shoaling predictions result.</p> <p>(This report uses a series of simple linear model equations applied in a finite element framework to develop guidance for the minimum mesh expansion rate, orientation, skewness, oscillation suppression, and bathymetric effects. While this effort was aimed at the TABS-2 modeling system, the findings are generally applicable to other finite element</p>					
20. DISTRIBUTION / AVAILABILITY OF ABSTRACT <input checked="" type="checkbox"/> UNCLASSIFIED/UNLIMITED <input type="checkbox"/> SAME AS RPT. <input type="checkbox"/> DTIC USERS			21. ABSTRACT SECURITY CLASSIFICATION Unclassified		
22a. NAME OF RESPONSIBLE INDIVIDUAL			22b. TELEPHONE (Include Area Code)		22c. OFFICE SYMBOL

OVER

10. WORK UNIT ACCESSION NO. (Continued).

Funding provided by Improvement of Operations and Maintenance Techniques research program Work Unit No. 32350, sponsored by the Headquarters, US Army Corps of Engineers.

19. ABSTRACT (Continued).

and finite difference models. Appendix A discusses the elimination of oscillations in the TABS-2 program.

PREFACE

This report is the product of research and development conducted from August 1988 through August 1989 in the Estuaries Division (ED), Hydraulics Laboratory (HL), US Army Engineer Waterways Experiment Station (WES), under the Improvement of Operations and Maintenance Techniques (IOMT) research program sponsored by the Headquarters, US Army Corps of Engineers (HQUSACE). Funding was provided under IOMT Work Unit No. 32350, "Estuarine Channel Maintenance by Training Structures."

Mr. R. C. Berger, Jr., ED, performed the work and prepared this report under the general supervision of Messrs. F. A. Herrmann, Jr., Chief, HL; R. A. Sager, Assistant Chief, HL; and Mr. W. H. McNally, Chief, ED.

The coordinator for the Civil Works Research and Development Program in the Directorate of Research and Development, HQUSACE, was Mr. J. A. Pfeiffer, Jr. HQUSACE Technical Monitor for the IOMT Program was Mr. J. Gottesman. The IOMT Program Manager at WES was Mr. R. F. Athow, Jr., ED. This report was edited by Mrs. M. C. Gay, Information Technology Laboratory, WES.

Commander and Director of WES during preparation of this report was COL Larry B. Fulton, EN. Technical Director was Dr. Robert W. Whalin.



Accession For	
NTIS GRA&I	<input checked="" type="checkbox"/>
DTIC TAB	<input type="checkbox"/>
Unannounced	<input type="checkbox"/>
Justification	
By	
Distribution/	
Availability Codes	
Dist	Avail and/or Special
A-1	

CONTENTS

	<u>Page</u>
PREFACE.....	1
PART I: INTRODUCTION.....	3
Background.....	3
Objectives.....	3
Approach.....	4
PART II: NUMERICAL BACKGROUND.....	5
The Shallow-Water Equations.....	5
Numerical Considerations.....	5
Background for Finite Elements.....	6
PART III: RESULTS AND DISCUSSION.....	11
Resolution.....	11
Orientation and Skewness.....	13
Oscillation Suppression.....	16
Bathymetric Effects.....	18
PART IV: CONCLUSIONS.....	21
REFERENCES.....	22
APPENDIX A: CONTROL OF OSCILLATIONS IN TABS-2.....	A1
Introduction.....	A1
Mixed Interpolation Stability Criteria.....	A1
Conclusions.....	A4
APPENDIX B: NOTATION.....	B1

CHANNEL MAINTENANCE BY TRAINING STRUCTURES: GUIDANCE
FOR NUMERICAL MODEL MESH DEVELOPMENT

PART I: INTRODUCTION

Background

1. Natural rivers and estuaries are quite shallow relative to their width; typical depth-to-width ratios are less than 1/10, which implies that the flow distribution is dominated by bottom friction rather than the drag from the channel banks (Chow 1959). Man-made training structures, however, are a sufficient anomaly in this environment to reverse the relative importance of these two. The training structure forces large velocity and water-surface gradients and, perhaps more importantly, severe changes in these gradients. Thus the structure will profoundly influence the flow pattern over a large region.

2. The complexity of the flow fields produced by training structures often precludes analyses short of physical or numerical modeling. Two-dimensional numerical models founded upon the shallow-water equations are common and are perhaps the simplest model capable of reasonably examining training structures. This report discusses the limitations of the numerical representation of these equations on applications with training structures.

3. The focus is upon the mesh development. Too often the factors in forming an adequate mesh are considered only after precision or stability problems are encountered, perhaps in final runs. A properly fabricated mesh from the onset will save time and expense avoiding costly reruns in a piecemeal fashion.

Objectives

4. The objectives of this investigation are to describe the influence of geometry and the mesh upon the precision of shallow-water numerical model results and to produce simple instructions and rules of thumb for mesh development. With this in mind, the following elements of mesh production are considered:

- a. Resolution.
- b. Mesh orientation.
- c. Skewness in the grid.
- d. Oscillation suppression.
- e. Bathymetric effects.

Approach

5. Assessments are made from a set of first-order linear model equations applied in a Galerkin finite element framework. All calculations are for steady model equations; therefore, no discussion of time discretization errors such as numerical dispersion is included. Steady models provide an uncomplicated method to evaluate grid-related problems. The first three items listed in paragraph 4 are resolved via the calculation of the truncation error in a one- or two-dimensional finite element model using a linear basis. The last two items are determined from the amplification caused by a one-dimensional finite element representation of a steady-state linearized shallow-water model.

PART II: NUMERICAL BACKGROUND

The Shallow-Water Equations

6. The shallow-water equations in one dimension may be written

$$H_t + UH_x + HU_x = 0 \quad (1)$$

$$U_t + UU_x = \nu U_{xx} - g(H + z)_x \quad (2)$$

where*

H = depth

t = time

U = velocity

x = distance

ν = apparent viscosity

g = acceleration due to gravity

z = channel bottom elevation

and the subscripts indicate differentiation. The basic assumptions in this formulation are mild bed slope and hydrostatic pressure distribution. The subsequent analysis is for steady flow conditions, which can be obtained from the previous equations by simply dropping the terms H_t and U_t . These equations can be derived from Euler's equations in a systematic fashion as in Stoker (1957).

Numerical Considerations

7. The numerical representation of the shallow-water equations can be subject to significant discretization errors, the introduction of which is a concern. The analytic solution of the differential equations (shallow-water equations) preserves the relationship among derivatives of variables specified by differential equations at EVERY point in the domain. The numerical model, on the other hand, is solved based upon a finite number of points. If the

* For convenience, symbols and unusual abbreviations are listed and defined in the Notation (Appendix B).

model is properly formulated, then as the number of mesh points increases to infinity, the analytic solution is recovered. This property is termed consistency.

8. As a result of the limited amount of information involved in a single equation, truncation error is introduced. In the case of a global expansion method, all data in the domain are used for each numerical equation, thus providing a low truncation error. In finite difference and finite element methods, only a limited number of neighboring points are used, reducing computational expense but producing much more truncation error. The truncation error associated with a particular numerical scheme is found by a Taylor series expansion of each nodal value about a common node location. In the following work, simple model equations are used to assess the truncation error in two spatial dimensions for linear basis using triangular and quadrilateral finite elements. The extension to finite difference is readily apparent. The following sections shall consider the truncation error of various finite element patches for a simple first-order model equation. Stability problems that may arise as a result of resolution and by the variation of bathymetry will then be discussed.

Background for Finite Elements

9. The Galerkin finite element technique as applied to differential equations will be approached through the idea of the approximation or interpolation of a function by some simpler set of functions. This in turn leads directly to application to differential equations in which relationships between the function and its derivatives are to be maintained. A variable such as concentration or velocity components can be approximated as a combination of functions. For example, the concentration $C(x)$ can be approximated as a linear function as

$$C(x) = a_1x + a_0, \text{ for } 0 \leq x \leq 1 \quad (3)$$

where a_0 and a_1 are constants. This can be rewritten equivalently as

$$C(x) = C_0(1 - x) + C_1x, \text{ for } 0 \leq x \leq 1 \quad (4)$$

where

$$C_0 = C(0)$$

$$C_1 = C(1)$$

are values at $x = 0$ and $x = 1$, nodal values. Equation 4 can then be simplified to the form

$$C(x) = \sum_{j=1}^2 \phi_j(x) C_j \quad (5)$$

where

$$\phi_1(x) = (1 - x)$$

$$\phi_2(x) = x$$

j = an index

It should be apparent that if a higher order approximation is desired, it is necessary only to include additional functions and corresponding nodal values. The particular type of function in Equation 5 is called a Lagrange polynomial; other function types can be developed, but these equations are in common use and will be used exclusively throughout this report. The functions used to approximate the variable $C(x)$ are termed interpolation or, alternatively, basis functions.

10. The finite element approach is to apply these interpolation functions over each element or region that subdivides the total region. In this manner the global solution can be approximated precisely without the need for a high-order polynomial. The total basis function for a node will then be the combination of functions for this node in all elements joining this node.

11. As an example of an application, consider the approximation of the function $\sin(x)$ over the interval $0 < x < \pi$ by linear polynomials. Only two elements will be used, though any number could be used. The approximation may be written as

$$C(x) = \sum_{j=1}^2 \phi_j[\xi(x)] C_j \quad (6)$$

where

$$\xi(x) = \frac{x - x_L}{x_R - x_L}, \text{ for } x_L \leq x \leq x_R \quad (7)$$

Within each element, L and R denote the left and right node locations.
The basis functions within the element are:

$$\phi_L(\xi) = 1 - \xi$$

$$\phi_R(\xi) = \xi$$

where ϕ is the one-dimensional linear shape function. To form the complete basis function ϕ_1 , for example, combine ϕ_R from element 1 with ϕ_L from element 2 (Figure 1).

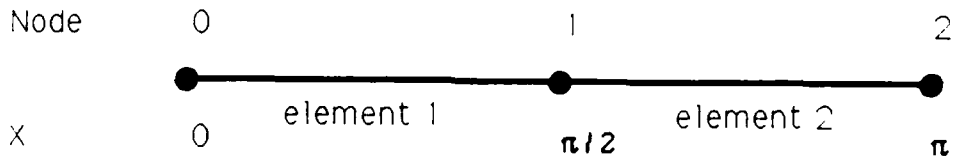


Figure 1. Finite element grid for approximation of $\sin x$

12. Further assume that $C_0 = C_2 = 0$, which precisely matches the function $\sin(x)$ at the boundaries and simplifies the problem of finding the proper value of C_1 . An obvious way to choose C_1 is again to simply let $C_1 = \sin(\pi/2) = 1$. The resulting approximation would be as shown in Figure 2.

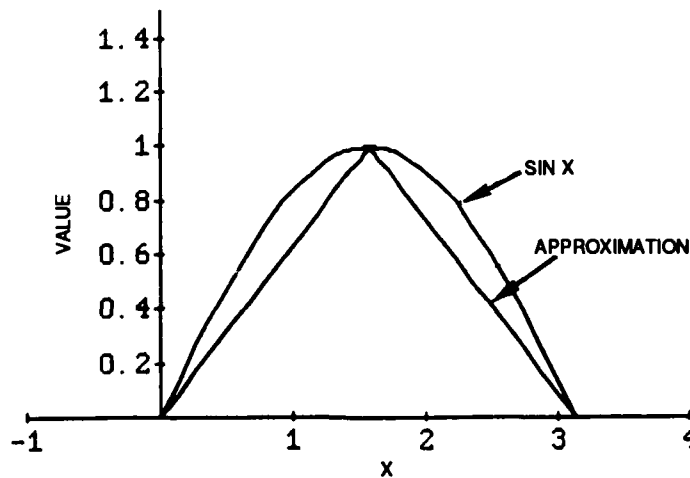


Figure 2. Direct interpolation

As one can see, this representation leaves something to be desired. It is consistently low. Another method would be to define error as $e = [f(x) - \sum_j \phi_j(x)C_j]$, where $f(x)$ is the function to be approximated ($\sin(x)$ in this case) and $\sum_j \phi_j(x)C_j$ is the approximate function. Minimize the error norm given by

$$\|e\| = \int_{\Omega} [f(x) - \sum_j \phi_j(x)C_j]^2 dx \quad (8)$$

where Ω is the domain, by taking the partial derivative with respect to each unknown C_j . The result is

$$\int_{\Omega} \phi_i(x) [f(x) - \sum_j \phi_j(x)C_j] dx = 0, \text{ for each } i \quad (9)$$

which is a set of algebraic equations to solve. An alternative way to write this is

$$(\phi_i, e) = 0 \quad (10)$$

where this is termed the inner product form. This indicates that the error is made orthogonal to the functions ϕ_i termed the test functions. Here it is shown that if the test functions are chosen to be the same as the interpolation or basis functions, the error is minimized. The result for the example is $C_1 = 1.216$. Figure 3 illustrates that this is a better choice than the previous case.

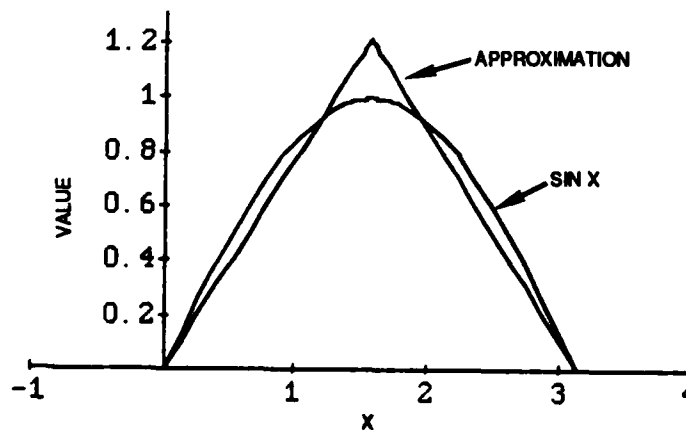


Figure 3. Galerkin approximation

The concept of using the same test functions as basis functions is the Galerkin technique in finite elements.

13. This technique needs to be applicable to differential equations. For example, consider the one-dimensional (1-D) steady-state convection diffusion equation

$$UC_x - DC_{xx} = 0 \quad , \text{ for } 0 < x < 1 \quad (11)$$

where D is the diffusion coefficient. Note that here the differential equation explicitly states a relationship between the function and its various derivatives. In this case there is a relationship between the function slope and curvature. The approximation needs to preserve this relationship as nearly as possible. The straightforward application is to let $C(x) = \sum_j \phi_j(x)C_j$. The Galerkin finite element approximation is then written as

$$[\phi_i, U \sum_j \phi_j'(x)C_j - D \sum_j \phi_j''(x)C_j] = 0 \quad , \text{ for each } \phi_i \quad (12)$$

where the prime indicates differentiation. This notation avoids subscripts j and x for different operations. It would appear that $\phi(x)$ must have at least second derivatives that are nonzero. However, $\phi(x)$ can be linear by using integration by parts putting a derivative on the test function. It should be noted that it can be shown that the Galerkin technique provides an "optimum" approximation when dealing with the function or any even-numbered derivatives. Unfortunately, in the case of the convection operator, which involves first derivatives only, there is no "norm" to be minimized by using the Galerkin technique. However, this technique is commonly used for convection problems as is the case in TABS-2.

14. The terms have been supplied that are necessary to understand the finite element examples, which follow.

PART III: RESULTS AND DISCUSSION

15. The steady-state shallow-water equations are often used to represent estuarine or riverine conditions in which convection is much more important than diffusion. Therefore a simple model equation that is only first order shall be considered:

$$f_x = 0 \quad (13)$$

This function can be thought of as convection of some species concentration f , in which the convection velocity has a value of 1 in the x -direction only. This example model equation will be used to evaluate 1-D and two-dimensional (2-D) model schemes.

Resolution

16. The resolution supported in a region determines the precision of the numerical results. However, there are few definitive suggestions about the grid size and the rate of expansion. In addressing the expansion rate question, consider the truncation error for the expansion of a 1-D finite element representation of $f_x = 0$. Representing this numerical equation in inner product form gives

$$(\phi_i(x), \sum \phi_j'(x) f_j) = 0, \text{ for all } i \quad (14)$$

The notation simply means the integral over the domain of the product of the two functions (separated by the comma). The function $f(x)$ is represented by an expansion in the basis function $\phi(x)$, i.e., $f(x) = \sum \phi_j(x) f_j$, and the prime indicates differentiation. The subscript indicates the nodal index, as shown in Figure 4. The inner product uses the same test function as that used as a basis for the function $f(x)$, thus a Galerkin weighted-residual statement.

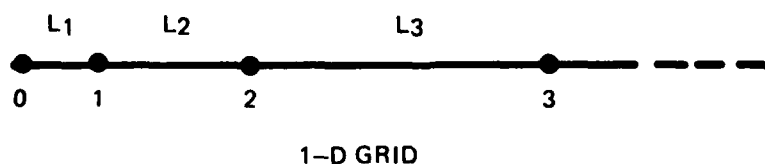


Figure 4. 1-D grid

17. If it is considered that the gradients in water levels and velocities and changes in gradients might be quite large at a dike, then the smallest elements need to be there. However, not being able to afford this resolution throughout the domain, the mesh size needs to be expanded in a prudent fashion such that the error would not be amplified severely. With this in mind, the truncation error associated with the boundary and at a typical location within the field shall now be considered. A single algebraic equation results from each selection of the test function $\phi_i(x)$. The function is nonzero only over the elements that contain node i . Thus, the equation includes only a few nodal values.

18. If $i = 0$ is chosen, then the algebraic equation associated with the boundary is selected. As implied by Figure 4, the basis chosen is linear with the resulting algebraic equation of

$$f_1 - f_0 = 0 \quad (15)$$

Expanding this expression in a Taylor series expanded about x_0 and solving for f_x gives the truncation error

$$\text{Truncation error} = -1/2 L_1 f_{xx} - 1/6 L_1^2 f_{xxx} - \dots \quad (16)$$

where L is the distance between adjacent nodes. Performing the same operations on a typical test function ϕ_i gives the algebraic equation and the truncation error

$$f_{i+1} - f_{i-1} = 0 \quad (17)$$

$$\text{Truncation error} = -1/2(L_{i+1} - L_i)f_{xx} - 1/6 \left(\frac{L_{i+1}^3 + L_i^3}{L_{i+1} + L_i} \right) f_{xxx} - \dots \quad (18)$$

Therefore, assuming f_{xx} at the boundary is greater than or equal to that out in the interior, if the element size varies as $L_i = iL_1$ (the element size increases such that the second element is length $2L_1$, the third $3L_1$, and so on), the precision in the mesh is no worse than that of the boundary.

Orientation and Skewness

19. Again considering the truncation error associated with a simple model problem $f_x = 0$, the 2-D finite element representation is investigated as either a set of triangles or quadrilaterals in the vicinity of a hypothetical dike. The simple model equation is analogous to the steady-state transport of f when the velocity is along the x-direction. This is completely general in that the coordinate system could be rotated to match the flow direction and result in this equation. Figure 5 illustrates this case.

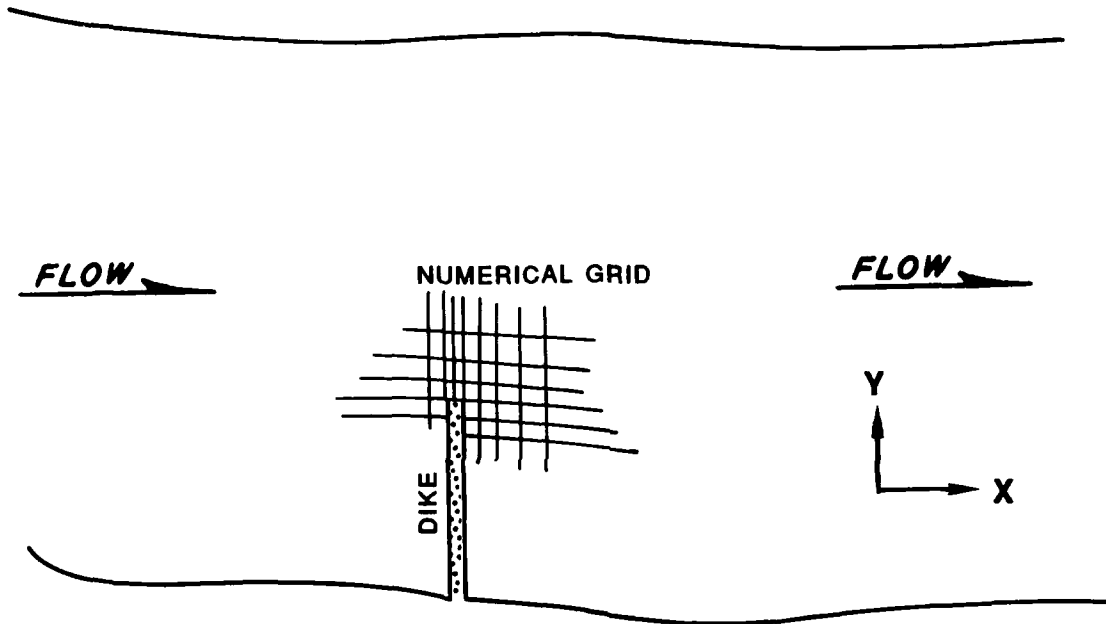


Figure 5. Schematized dike in a flow field

The flow is in the x-direction and the dike is perpendicular to the flow, i.e., in the y-direction. Note that downstream of the dike tip very large derivatives are expected in the y-direction but not in the x-direction. Thus a truncation error in which only y-derivatives are present will be emphasized.

20. The finite element statement and the region or patches over which it will be applied are as follows:

$$(\phi_i(x,y), \sum \phi_j'(x,y)f_j) = 0, \text{ for each } i \quad (19)$$

where

ϕ = 2-D linear basis functions, either triangle or quadrilateral elements

' = partial derivative with respect to x

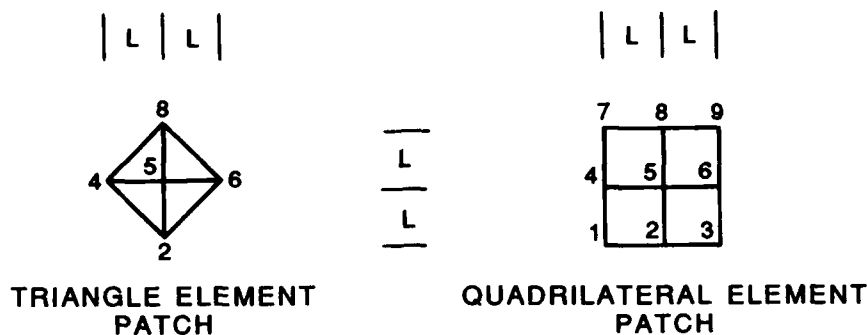


Figure 6. Typical 2-D finite element patches

The patches shown in Figure 6 result from the nonzero region of the test function ϕ_5 . This is the only region that needs to be considered since in the finite element method when $i = 5$, the product of this test function is being integrated with the partial differential equation and so the only contribution to the resulting algebraic equation is from the nonzero region of the test function ϕ_5 , as shown in the following equations:

a. Triangles:

$$(f_6 - f_4)(Y_8 - Y_2) + (f_2 - f_8)(Y_6 - Y_4) = 0 \quad (20)$$

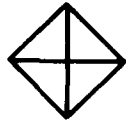
b. Quadrilaterals:

$$\begin{aligned} f_1(Y_2 - Y_4) + f_2(-Y_1 + Y_3 - Y_4 + Y_6) + f_3(-Y_2 + Y_6) + f_4(Y_1 \\ + Y_2 - Y_7 - Y_8) + f_5(-Y_2 - Y_3 + Y_8 + Y_9) + f_7(Y_4 - Y_8) \\ + f_8(Y_4 - Y_6 + Y_7 - Y_9) + f_9(-Y_6 + Y_8) = 0 \end{aligned} \quad (21)$$

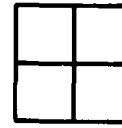
where Y is distance normal to the x-axis.

21. These algebraic equations can be used to calculate the truncation error by expanding in a Taylor series about the location of node 5. It is assumed for simplicity that the metrics involved in the geometric transformation are exact. In this manner, Figure 7 was developed showing the truncation error for the triangular- and quadrilateral-based finite element patches under three circumstances.

22. Figure 7a indicates the truncation error for the case in which both grids form an orthogonal patch oriented with the flow. The truncation error of the quadrilateral patch includes an additional term beyond that of the

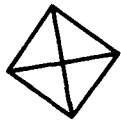


$$-1/6 L^2 f_{xxx}$$



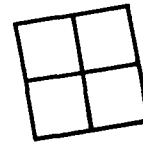
$$-1/6 L^2 (f_{xxx} + f_{xyy})$$

a. Oriented with the flow



α

$$-1/6 L^2 (f_{xxx} + 3\alpha f_{xxy} - \alpha f_{yyy})$$



α

$$-1/6 L^2 (f_{xxx} + f_{xyy})$$

b. Possible rotation

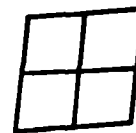
0.5α



0.5α

$$-1/6 L^2 (f_{xxx} + 3\alpha f_{xxy} - \alpha f_{yyy})$$

0.5α



0.5α

$$-1/6 L^2 (f_{xxx} + 2\alpha f_{xxy} + f_{xyy})$$

c. Skewness

Figure 7. Leading terms of truncation error for $f_x = 0$

triangular mesh. It is not a term f_{yyy} ; thus the truncation error is probably small for both cases (remember that gradients in the x-direction are small). Possible rotation is shown in Figure 7b, and skewness (collapse of the element) in the patch is shown in Figure 7c. Both cases deal with a small rotation or skewness angle of α , where $0 < \alpha \ll 1$.

23. The inclusion of a slight rotation results in two additional terms in the truncation error of the triangular case. More importantly, one of these terms involves f_{yyy} , which could be quite large in the vicinity of the dike tip. The quadrilateral patch, on the other hand, had no change in truncation error for this condition.

24. The effect of a small degree of skewness was identical to the small rotation for the triangular patch, including the potentially large term f_{yyy} . The quadrilateral patch with this slight skewness was changed to include an additional term f_{xxy} .

25. It may then be concluded that for best results, grids in the vicinity of the dike tip should be aligned with the flow direction and orthogonal. If this is not possible, it would be preferable to use quadrilateral elements in this immediate vicinity.

Oscillation Suppression

26. A common problem with shallow-water numerical models is the appearance of spatial oscillations around steep changes in the flow variables. This is actually a problem in transport models as well and results from the first-order derivatives in the differential equations. To illustrate the problem, consider the case of the steady convection-diffusion equation

$$Uf_x = Df_{xx} \quad (22)$$

where

U = convection velocity

x = coordinate direction

Subscripts indicate differentiation with respect to x . Representing f as discrete nodal values in a linear basis gives

$$f(x) = \sum_j \phi_j(x) f_j \quad (23)$$

where ϕ is the interpolation function. The algebraic equation set resulting from the Galerkin finite element representation of the convection diffusion equation for a linear basis and a uniform grid is

$$(f_{j+1} - f_{j-1}) + \frac{2}{R} (f_{j+1} - 2f_j + f_{j-1}) = 0 \quad (24)$$

where $R = UL/D$ and is known as the Peclet number or the cell Reynolds number. If it is assumed that

$$f_j = c\rho^j \quad (25)$$

where

$c = \text{a constant}$

$\rho = \text{the numerical root}$

there are two roots $\rho = 1$, $(2/R - 1)/(2/R + 1)$. The first root implies that f is a constant; the second, however, allows variability in f . But note that if ρ is negative, the model representation will oscillate. Thus it must be noted what restrictions guarantee that ρ will be positive. Limiting the minimum value to zero, the relationship to prevent oscillation in the model is

$$R = UL/D < 2 \quad (26)$$

Therefore, it is possible to refine the grid to prevent oscillations, provided the diffusion is not negligible.

27. The extension to the shallow-water equations is not straightforward as there is a set of equations, one of which (conservation of mass) contains no diffusion term at all. Therefore, there is no means to damp water-surface oscillations in a model using linear basis for both water-surface and velocity. It has been shown (Platzman 1978, Walters and Carey 1983) that by using a mixed interpolation (quadratic for velocity and linear for water surface) the 2L wavelength oscillation does not appear in the water surface. This representation is used in many shallow-water models, in particular, the TABS-2 hydrodynamic model RMA-2V (Thomas and McAnally 1985). The velocity

oscillation is controllable via the diffusion and mesh resolution. The relationship for small Froude number, $F = U/(gH)^{1/2}$, reverts to the same relationship found for the convection-diffusion model (for details see Appendix A)

$$R = \frac{UL}{\nu} < 2 \quad (27)$$

where L is the distance between velocity nodes. In the 2-D case, it is important to note that the streamwise diffusion or viscosity and resolution are the important parameters in suppression of oscillations. It should also be noted that while the $2L$ wavelength oscillation in the water surface will be suppressed, longer wavelength oscillations can occur.

Bathymetric Effects

28. In model applications, numerical model behavior appears to be much less stable when the bathymetry changes rapidly. Limitations are imposed by the model equations themselves due to the mild slope assumption and the lack of variation of velocity over depth. However, this instability is in fact numerically induced.

29. In addition to the oscillation suppression by diffusion and resolution discussed previously, which were evaluated for flat bottom conditions, a variable bathymetry must now be considered. The problem will be simplified by excluding viscosity and using linear basis for both water surface and velocity, the reasoning being that the purpose of this exercise is illustrative, and can be accomplished even without these additional complications.

30. The 1-D steady-state shallow-water equations may be written as:

$$UH_x + HU_x = 0 \quad (28)$$

$$gH_x + UU_x = -gz_x \quad (29)$$

where U is the longitudinal velocity. These equations can be linearized by considering small perturbations about a solution. An obvious solution of this set of equations is that the water surface is flat and that the velocity is zero, or

$$H + z = \text{Constant} \quad (30)$$

$$U = 0 \quad (31)$$

A perturbation about this solution can be represented as

$$0 < u \ll 1$$

$$0 < h \ll 1$$

where u and h are the perturbation quantities. Dropping all terms involving products of the perturbation quantities, the resulting linearized equations are

$$uH_x + Hu_x = 0 \quad (32)$$

$$gh_x = 0 \quad (33)$$

The solution to these equations is straightforward. Certainly h is a constant, and u can be determined by supplying a depth variation. Assume

$$H(x) = H_0 \xi^{x/L} \quad (34)$$

so that every shift of a distance L along x results in the depth being multiplied by ξ (the subscript o indicates the value at the origin). Therefore, the solution is

$$u(x) = U_0 \xi^{(-x/L)} \quad (35)$$

31. The question now becomes, what is the numerical solution to this same problem? Again using a linear basis for Galerkin finite elements and assuming a numerical solution of the form:

$$u_j = U_0 \rho^j \quad (36)$$

the roots are found to be

$$\rho = 1/\xi, \quad \frac{-(2 + \xi)}{(1 + 2\xi)} \quad (37)$$

The first root matches the analytic result at the nodes. The second root is a numerical artifact; and since it is negative, a node-to-node oscillation results. Consider the roots shown in Figure 8.

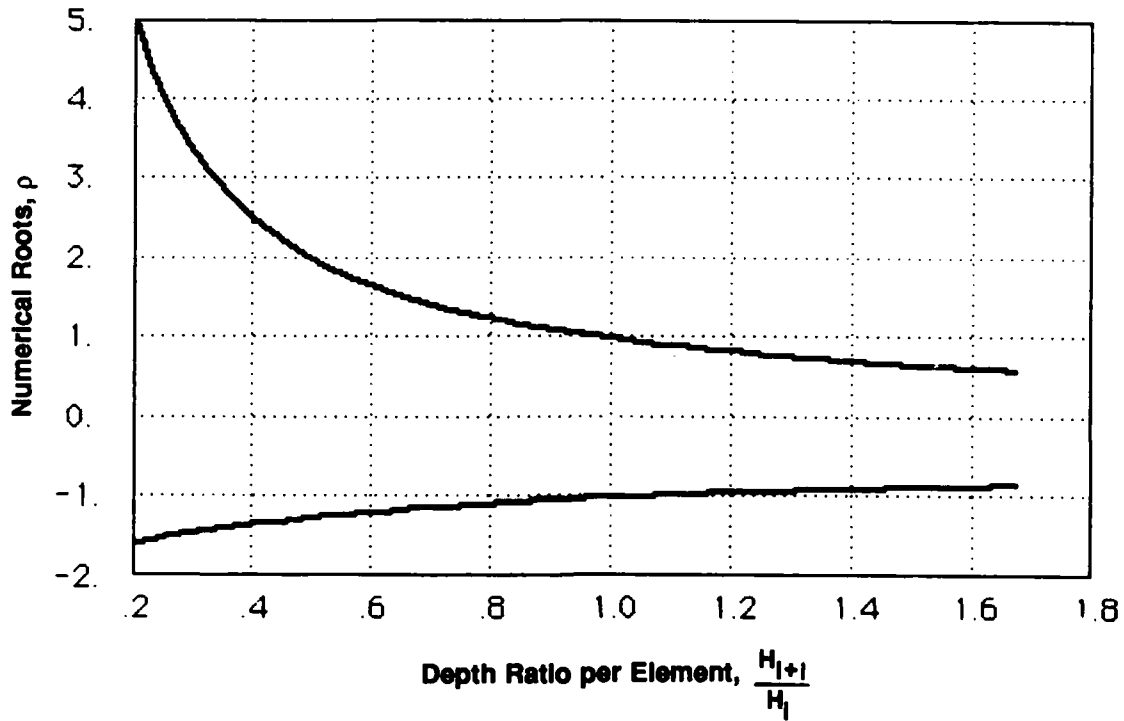


Figure 8. Depth sensitivity

The upper curve is the actual root and the lower curve the spurious root. For flat bottom channels, $\xi = 1$ and the spurious root for $\xi = 1$ is $\rho = -1$. If the flow deepens in the direction of flow, corresponding to $\xi > 1$, ρ is less than 1 and the oscillations will be dampened. However, if the depth decreases in the direction of flow, $\xi < 1$, the oscillations will be amplified, possibly resulting in the model becoming unstable. Therefore, flows in a direction of decreasing depth will be prone to instability and will require additional resolution for the same diffusion coefficient.

PART IV: CONCLUSIONS

32. The precision and stability of a given numerical model depend heavily upon the associated computation mesh. When large gradients are generated by the inclusion of training structures, grid-related problems are magnified. The following guidance is noted:

- a. A rule of thumb for the element expansion rate as one moves away from a structure is $L_i = iL_1$. That is, the element adjoining the boundary is L_1 , the next element out is of size $2L_1$, the third is $3L_1$, and so on.
- b. Near the dike tip, it is important to orient the grid with the flow direction and make the elements as nearly orthogonal as possible.
- c. Quadrilateral elements appear to be more forgiving than triangular ones in cases in which the orientation and skewness are more extreme.
- d. Oscillations in shallow-water models employing the mixed interpolation with linear water surface and quadratic velocity will have oscillations if $UL/\nu > 2$. While $2L$ wavelength oscillations in water surface should not occur, oscillations with longer wavelengths are possible, possibly leading to misleading conclusions.
- e. Depth decreasing in the direction of flow renders the model less stable; the converse is true for depth increasing.

REFERENCES

- Chow, V. T. 1959. Open Channel Hydraulics. McGraw-Hill, New York, pp 26-27.
- Platzman, G. W. 1978. "Normal Modes of the World Ocean; Part 1, Design of a Finite Element Barotropic Model," Journal of Physical Oceanography, Vol 8, pp 323-343.
- Thomas, W. A., and McAnally, W. H. 1985. "User's Manual for the Generalized Computer Program System: Open-Channel Flow and Sedimentation, TABS-2," Instruction Report HL-85-1, US Army Engineer Waterways Experiment Station, Vicksburg, MS.
- Stoker, J. J. 1957. Water Waves: The Mathematical Theory with Applications. Interscience Publishers, New York, pp 27-32.
- Walters, R. A., and Carey, G. F. 1983. "Analysis of Spurious Oscillation Modes for the Shallow Water and Navier-Stokes Equations," Journal of Computers and Fluids, Vol 11, No. 1, pp 51-68.

Introduction

1. A common problem in numerical models involving transport is the presence of oscillations ("wiggles") in the solution. This is a direct result of the numerical method as applied to a first-order differential equation (any odd number order actually). Often some form of mixed interpolation is used to alleviate this problem (TABS-2, for example). In the case of the shallow-water equations, the water surface or depth is interpolated linearly and the velocity is quadratic. It has been shown (Platzman 1978; Walters and Carey 1983)* that this will have a node-to-node oscillation in the velocity field but not in the water surface; thus, including viscous effects in the momentum equation can control this. (Note that if the water surface has oscillations, there is no mechanism to control this with a standard Galerkin scheme.) These analyses, however, did not include viscous effects in the calculation.

2. This appendix calculates the necessary viscosity to eliminate oscillations in a mixed interpolation finite element model of the one-dimensional (1-D) shallow-water equations and the conditions under which oscillation in water surface may be present.

Mixed Interpolation Stability Criteria

3. The discrete equations resulting from the Galerkin weighted-residual statement of the 1-D shallow-water equation using mixed interpolation are as follows**:

a. Conservation of mass:

$$3U_0(-h_1 + h_5) + h_0(-u_1 - 4u_2 + 4u_4 + u_5) = 0 \quad (A1)$$

* References cited in this appendix are included in the References at the end of the main text.

** For convenience, symbols and unusual abbreviations used in this appendix are listed and defined in the Notation (Appendix B).

b. Conservation of momentum:

$$g(-h_1 + h_5) + U_o(u_1 - 4u_2 + 4u_4 - u_5) + \frac{\nu}{d} (2u_1 - 16u_2 + 28u_3 - 16u_4 + 2u_5) = 0 \quad (A2)$$

$$g(-h_1 + h_3) + U_o(-u_1 + u_3) + \frac{\nu}{d} (-4u_1 + 8u_2 - 4u_3) = 0 \quad (A3)$$

and a similar equation to A3 centered about node 4

where

U_o, h_o = a solution of the shallow-water equations in which U_o and h_o are constants

h, u = perturbation quantities

g = acceleration due to gravity

ν = apparent viscosity

d = length of an element

These equations are for perturbation equations about the solution

$$u = U_o \quad (A4)$$

$$h = h_o \quad (A5)$$

on the typical finite element patch, as shown in Figure A1.

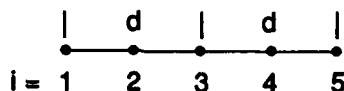


Figure A1. Finite element patch

All other subscripts indicate nodal values. Here the elements contain three nodes; u is nodally defined at all three nodes while h is defined only at the end nodes (knots). Equations A1 and A2 result from the weight function for node 3 applied against the conservation of mass and momentum equations, respectively. Equation A3 is the result of the test function for node 2 applied to the conservation of momentum equation. A similar equation results from the application of the test function at node 4; however, as those elements are uniform, this equation is identical to Equation 3 shifted one

element. Note then that there are three equations within this patch enforcing momentum relationships and only one for conservation of mass. This is a direct consequence of the mixed interpolation and the use of the Galerkin method. Write the nodal values as

$$u_j = \hat{U}_\rho^j \quad (A6)$$

$$h_j = \hat{h}_\rho^j \quad (A7)$$

where ρ is a numerical root, which may be complex, and \hat{U} and \hat{h} are arbitrary constants. Making these substitutions and finding the solutions to Equations A1-A3 for which $\hat{U} = \hat{h} \neq 0$ yields the expressions:

$$\begin{aligned} & \left[\left(3F^2 - 6\frac{F^2}{R} - 1 \right) \left(9F^2 - 21\frac{F^2}{R} - 5 \right) + \left(3F^2 - 3\frac{F^2}{R} + 1 \right) \left(3F^2 + 6\frac{F^2}{R} - 5 \right) \right] \rho^2 \\ & + \left[\left(3F^2 - 6\frac{F^2}{R} - 1 \right) \left(9F^2 + 21\frac{F^2}{R} - 5 \right) + \left(3F^2 - 3\frac{F^2}{R} + 1 \right) \left(3F^2 - 6\frac{F^2}{R} - 5 \right) \right] \rho \\ & + \left[\left(3F^2 - 3\frac{F^2}{R} + 1 \right) \left(3F^2 + 6\frac{F^2}{R} - 1 \right) - \left(3F^2 - 6\frac{F^2}{R} - 1 \right) \left(3F^2 + 3\frac{F^2}{R} + 1 \right) \right] = 0 \quad (A8) \end{aligned}$$

$$\rho = 1 \quad (A9)$$

where F is the Froude number and R is the Peclet number. The second expression (A9) is simply the statement that a constant U_j and h_j is a solution. Here,

$$F^2 = \frac{U_o^2}{gh_o} \quad (A10)$$

$$R = \frac{U_o d}{2\nu} \quad (A11)$$

where d is the length of an element, which corresponds to $2L$ from paragraph 27, main text. Equation A8 then represents potential artificial solutions. The equation is resolved by realizing that most estuary and river applications involve flow conditions characterized by small Froude numbers. Thus considering $0 < F \ll 1$, the perturbation equation is derived:

$$\left(-1 + \frac{2}{R}\right) \rho^2 + \left(-1 + \frac{1}{2R}\right) \rho + \frac{1}{2R} = 0 \quad (A12)$$

From this analysis one can show that if $R = 2$, a node-to-node oscillation is possible in the velocity field. However, the water surface will contain no oscillation. Thus it is desirable to have $R \leq 2$, which is essentially identical to the well-known cell Peclet criterion for linear basis.

4. If the cell Reynolds number drops to $1/2$, an oscillation of wavelength $2d$ is possible. Note that this corresponds to an oscillation in water surface as well as velocity. The amplitude is small for this mode, but an oscillation in the linearized model will exist in water surface.

Conclusion

5. To avoid oscillations in TABS-2 model results, one should make sure that

$$R = \frac{U_o d}{2\nu} < 2 \quad (A13)$$

This also states that higher flow rates will require increased eddy viscosity.

6. It is possible to have an oscillation in the water surface even without including nonlinear effects.

APPENDIX B: NOTATION

C	Concentration
d	Length of an element
D	Diffusion coefficient
e	Error
f	Concentration
f_j	Nodal value of f
F	Froude number
g	Acceleration due to gravity
H	Depth
j	Node index progressing in the x -direction
L	Distance between adjacent nodes
R	Peclet number or cell Reynolds number
t	Time
u, h	Perturbation quantities
U	Velocity
U_0, h_0	Solution of the shallow-water equations in which U_0 and h_0 are constant
x	Distance coordinate direction
Y	Distance normal to x -axis
z	Channel bottom elevation
α	Angle
ν	Apparent viscosity
ρ	Numerical root
ϕ	One-dimensional linear shape function
Φ	Two-dimensional linear basis functions, either triangular or quadrilateral elements
Ω	Domain